51st AIAA/ASME/ASCE/AHS/ASC Structures, Structural Dynamics, and Materials Conference<BR> 18th
12 - 15 April 2010, Orlando, Florida

AIAA 2010-2997

# A Simulation-based Design Model for Analysis and Optimization of Multi-State Aircraft Performance

Jeremy S. Agte*
*Massachusetts Institute of Technology, Cambridge, MA*

Nicholas K. Borer†
*The Charles Stark Draper Laboratory, Cambridge, MA*

Olivier de Weck‡
*Massachusetts Institute of Technology, Cambridge, MA*

**This paper introduces an approach to aircraft design and analysis that focuses on the evaluation of aircraft as multi-state systems, where a multi-state system is one having a finite set of performance levels or ranges, differentiated in this case by distinct levels of failure. In order to accurately examine numerous aircraft performance states, a multi-disciplinary design model was used, consisting of an open-source 6-DoF flight simulator integrated with a vortex lattice aerodynamics solver and a MATLAB routine for calculation of weights and inertias. The primary impetus for using a flight simulator run in batch mode was to facilitate a global approach for concurrent analysis of aircraft expected performance and availability. Namely, by allowing systematic calculation of performance metrics for differing aircraft states, the relationship between an aircraft's global design variables and its performance and availability may be established. Such an approach allows designers to identify those elements that might drive system loss probability through an analysis of performance changes across system states and their respective sensitivity to design variables.**

## Nomenclature

| | | | |
|---|---|---|---|
| $\Gamma$ | Dihedral | $C_{m\alpha}$ | Change in pitch moment coeff. with AOA |
| $\Lambda$ | Wing sweep | $C_{mq}$ | Change in pitch mom. coeff. with pitch rate |
| $\lambda$ | Taper ratio or (with subscript) component reliability | $C_{n\beta}$ | Change in yaw moment coeff. with sideslip |
| | | $C_{nr}$ | Change in yaw moment coeff. with yaw rate |
| $b$ | Wing span | $C_{Yr}$ | Change in sideforce coeff. with yaw rate |
| $C_{D\delta e}$ | Change in drag coeff. with elevator defl. | $E_A$ | Expected system availability |
| $C_{l\beta}$ | Change in roll moment coeff. with sideslip | $E_G$ | Expected performance |
| $C_{L\delta f}$ | Change in lift coeff. with flap deflection | $G_k$ | Performance in state k |
| $C_{l\delta r}$ | Change in roll mom. coeff. with rudder defl. | $p_k$ | Probability of being in state k |
| $C_{lp}$ | Change in roll moment coeff. with roll rate | $S_k$ | State k |

## I. Introduction

TODAY'S increasingly complex systems are expected to operate in a wide array of environments and conditions. This is particularly true of aircraft, where long design cycles and operational lifetimes virtually guarantee that the system will perform in a variety of scenarios that may or may not have been

*Major, USAF, Ph.D. Candidate, MIT Aero/Astro Dept., Cambridge, MA, AIAA Senior Member.
†Systems Design Engineer, Charles Stark Draper Laboratory, Cambridge, MA, AIAA Member
‡Associate Professor, Dept. of Aeronautics and Astronautics, Engineering Systems Div., AIAA Associate Fellow

considered during the original development program. In addition, aircraft often experience growth in their descriptive parameters as technologies change throughout the their operational life. Each potential system and operational configuration must further demonstrate adequate reliability and survivability behavior, in which the contingency performance metrics of the system must be considered in a variety of degraded modes.

Design optimization of aircraft largely focuses on the system in a nominal configuration, with constraints in place for off-nominal conditions as a way of handling the degraded modes as mentioned above. This approach has largely been successful because of our long experience with aircraft design; the off-nominal scenarios that exist are well-characterized. Yet, certification of an aircraft still remains a daunting (and expensive) endeavour to prove that the system exhibits acceptable performance in the event of such a scenario. Design decisions made years before in the name of nominal performance or cost may lead to unacceptable off-nominal performance, especially in cases where it is too difficult to analyze early on, or when new technologies are involved and the failure modes and mechanisms are not well understood. In the former case, one needs to look only as far as spin-testing of certified aircraft to see examples of expensive (and time-consuming) fixes made in the name of an unlikely off-nominal scenario.[1]

Advances in aircraft capabilities limit the applicability of our previously well defined off-nominal scenarios. Unmanned Aircraft Systems (UAS) are becoming far more prevalent in the military and civil applications. Solid-state flight instruments and controls are replacing analog "steam gauges" and cable-and-pully control systems in manned and unmanned aircraft. Increasing automation and endurance are more common in aircraft designed for tomorrow's environments. Properly integrated, these technologies provide radical increases in mission diversity of aircraft, but they also bring about new, unexpected failure modes that challenge the status quo. A UAS must be able to respond properly, and often without human intervention, in the presence of a failure, maintaining safety in what may be a highly congested corner of airspace. Automatic error-checking algorithms cross-checking different sensors must be thoroughly tested, lest a bad value be used to feed into a control algorithm. As systems become more autonomous, very long-endurance missions become possible, and systems must be designed from the outset to be exceptionally reliable and to operate in the presence of failed equipment. Complicating this fact, aircraft do not have the availability of a benign "safe mode" as their long-endurance spacefaring cousins. These and other cases suggest that it may no longer be sufficient to conduct typical, constrained nominal-case optimization during aircraft design.

This article is the first of a series to describe a novel approach to system design that considers multiple states of a system earlier in the design process. The authors propose a multi-state system formulation that is capable of capturing system behavior in much more than just a nominal state. This will be tested on a detailed, integrated model of a well-understood problem - that of the design and failure analysis of a typical twin-engine aircraft. A well-known problem is used as the behavior of its failure modes is understood, and should be uncovered by the multi-state approach. This paper describes the simulation-based model developed for general multi-state aircraft analysis and begins exploration of the multi-state design space. Future work will further develop these multi-state methods by leveraging this model.

## II. Multi-State System Modeling

Although multi-state system modeling has been applied to aircraft design, the majority of this work has been in the area of flight controls and software development. Focus has been on detecting and compensating for failure and damage of flight control effectors and in many cases using the remaining functional effectors to create compensating forces and moments.[2] Selected cases have even developed and tested emergency control laws for completely failed systems using only differential thrust,[3] or retrofitted adaptive control systems to existing flight software.[4] In constrast, the work presented in this paper focuses not directly on the control system, but on the aircraft's up-front design variables from a multi-state perspective. In both areas, the multi-state approach has its roots in analysis of system failures, where the two major enabling pieces have their roots in system reliability or availability analysis. These two major enablers are behavioral-Markov modeling and expected value sensitivity.

### A. Behavioral-Markov Modeling

Draper Laboratory has a history of using integrated system modeling with Markov models to determine system reliability for life-critical applications and large, complex systems.[5,6] Markov analysis ensures that highly improbable events and sequences of these events are accurately measured and tracked, which may

otherwise be overlooked with Monte Carlo analysis due to their extremely low probability of occurrence. In practice, the Markov model construction is incorporated with an integrated system model, allowing the user to enumerate the dependency structure of the individual components. This capability ensures that dependent failures or cascading effects are adequately represented in the reliability estimates, which have not typically been sufficiently captured through traditional reliability estimation techniques.[7]

This investment in the capability for system reliability analysis has been recently expanded by merging system behavioral analysis with the integrated Markov model generation. The approach allows the evaluation of system performance for multiple system events (i.e. multiple failure modes and/or sequences of failures), and has been demonstrated by Draper-sponsored university research,[8,9,10] NASA-funded projects,[11] and commercially-funded programs. A behavioral-Markov modeling approach provides the ability to capture both the flow of probability through multiple system states (brought on by various failure sequences) and the associated degraded system performance. The user provides a system behavioral model, describes the individual failure modes available to each of the constituent elements, and builds the Markov model from this information. Each Markov state represents a single run of the behavioral model, which captures the system performance metrics. These metrics are compared to performance bounds for the operation, from which the state is classified as operational, mission loss, system loss, etc.

A notional behavioral-Markov model is provided in figure 1. In this formulation, the probability $p_k$ that the system finds itself in any particular state $k$ of performance $G_k$ at time $t$ can be determined by solving a system of first order linear differential equations derived from the transition probabilities. These transition probabilities are typically derived from known values of component or element *mean-time between failures (MTBF)*. The simplest formulation for the failure rate of the $i^{th}$ component, $\lambda_i$, is simply the inverse of the MTBF. The performance $G_k$ can be compared to bounds on system performance, enabling classification of each Markov state as system loss, mission loss, and so on. From here, calculation of reliability, availability, mission success probability, or any other aggregate probabilistic metric is simply a matter of summing the Markov probabilities that are within the appropriate bounds (this is expanded upon below).

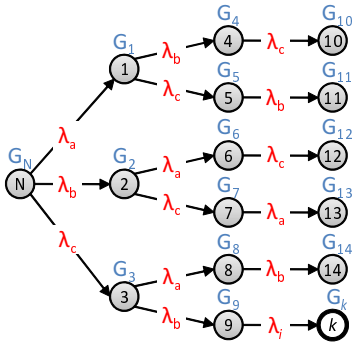


**Figure 1. Markov Chain Formulation**

## B. Availability and Expected Performance

The behavioral-Markov approach enables far more than system reliability analysis. Properly generalized, it allows for the rigorous enumeration of the performance associated with any probabilistic sequence of discrete events. While the user has to understand the impact of these singular events, they only need to model the effects on the initiating element. The integrated behavioral model then captures the cascading effects through the whole system. The Markov model will generate all possible event sequences (to a user-specified number of random events) and the behavioral model will capture the performance as it cascades through the integrated system for each particular event sequence.

As described above, if each performance level $G_k$ can be determined, it is possible to determine aggregate measures of probabilistic system performance. Two metrics of interest are the system's overall availability $E_A$ and expected performance $E_G$ according to equations 1 and 2, taken from Levitin and Lisnianski.[12] Here, $T$ represents a designated period of time, often divided into $M$ intervals of $T_M$ where each interval may have its own acceptable minimum performance level $W_M$. $A(W_M)$ is the summed probabilities of those states that have achieved $W_M$ in time interval $T_M$.

$$E_A = \sum_{m=1}^{M} A(W_M)\frac{T_M}{T} \quad \text{where} \quad A(W_M) = \sum_{G_k \geq W_M} p_k \tag{1}$$

$$E_G = \sum_{k=1}^{K} p_k G_k \tag{2}$$

While each of these metrics is useful in its own right, they are far more powerful when combined with system sensitivity analysis. Namely, it is desirable to know how these quantities change as system parameters

are modified. This approach has been used in the past for system reliability analysis.[6,11] In these cases, the absolute system reliability was of less concern than identifying those elements that drive the system loss probability. These elements were discovered through sensitivity analysis, solving equation 1 for $i = k$ number of cases, where each case modified the failure rate of the $i^{th}$ component. The components that drive system loss will be those that exhibit the largest sensitivity, or change in $E_A$ given a change in $\lambda_i$. This sensitivity is not necessarily used for direct optimization - it is elementary to know that reducing a component failure rate will (generally) increase reliability - rather, it is used to point the system designers to the portion of the system architecture that has the greatest effect on reliability. The remedy may lie with finding a higher-reliability component, introducing redundancy, changing the mission parameters, or a host of other solutions.

System sensitivity analysis can be extended to the expected performance values $E_G$. In this way, it should be possible not only to observe sensitivity of the expected performance to component failure rates, but also traditional aircraft design variables (wing span, wing area, etc.) and operational parameters (cruise altitude, cruise speed, etc.). The individual Markov state probabilities $p_k$ act as "weights" to a weighted performance equation. Hence, for short missions, where there is little chance for the system to enter any but the nominal state, expected performance sensitivity will look much like a standard design sensitivity analysis. However, as system lifetime increases, the probability of the off-nominal Markov states will increase, which will tend to change the expected performance sensitivity. Hence, expected performance sensitivity appears to be a promising metric to identify those system parameters that have the greatest effect on both nominal and off-nominal system performance.

## III. Aircraft Integrated System Model

The design problem for the case under study here is divided into an *aspect* oriented hierarchy with sub-disciplines of *weights and inertias*, *aerodynamic forces and moments*, *propulsion*, and *performance*. Figure 2 shows a simplified depiction of the design model information flow. All geometry is entered as basic aircraft design variables such as aspect ratio, taper ratio, wing sweep, fuselage height and width, engine location, etc., which are used to calculate weights and inertias for the aircraft's various components. These geometric parameters are also passed to a preprocessor for input to the vortex lattice code as geometric coordinates for discretized lifting surface panels. A few of the geometric parameters are handled directly by the flight simulator executable in the *performance* module, such as the location of the fuel tanks, so that the inertial effects of fuel burn may be directly accounted for during run-time. The dotted lines in the feedback from *performance* to *weights and inertias* and *aerodynamic forces & moments* indicate the potential effect of engine size and weight on these two disciplines. They are not linked in the current model at this stage since the analysis in this study assume a specific engine that does not vary in maximum thrust or size.

### A. Disciplines

The *weights and inertias* discipline computes various component weights using empirically based equations from Brandt et al.[13] and Raymer.[14] Intertias are then calculated for each of these components by discretizing them into smaller divisions, computing the divisional centers of gravity and mass, and then summing the respective inertias to get $I_{xx}$, $I_{yy}$ and $I_{zz}$ for the wing, tail, fuselage, etc. Each component value is passed to the *aerodynamic forces and moments* module, where total vehicle inertias are used to help determine the aircraft's response characteristics. All of the code in the *weights and inertias* discipline is written in Matlab.

A vortex lattice solver is used in the *aerodynamic forces and moments* discipline. This is the publicly available GNU licensed Athena Vortex Lattice (AVL), which employs an extended vortex lattice model for lifting surfaces and a slender body model for fuselages and nacelles.[15] Athena Vortex Lattice is written in Fortran and takes as input the aircraft geometry coordinates (which in this case have been processed from the aircraft geometric design variables) and specified mass properties. Output data are all of the aircraft control derivatives passed to the JSBSim *performance* module shown in figure 2. This is also where the aircraft's drag polar is calculated, providing both $C_L$ and $C_D$ as a function of angle-of-attack. Lift and drag characteristics for various flap configurations (leading or trailing edge) may be computed as a function of angle-of-attack as well. These may be determined for any aircraft geometry coming out of the aerodynamics module and then used in the *performance* simulation to model various in-flight configuration changes.

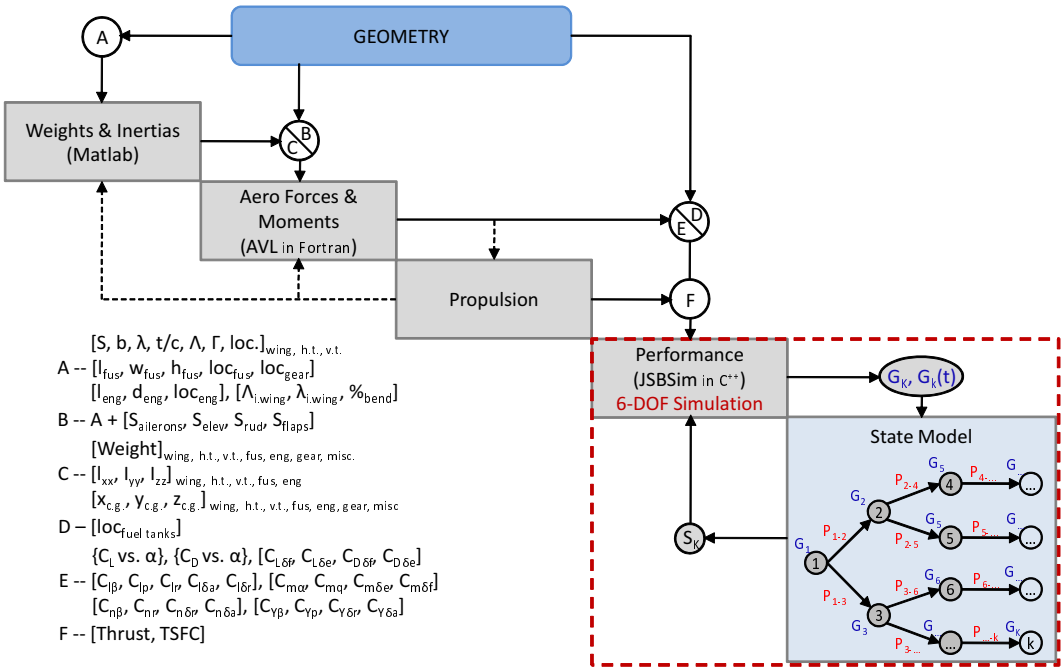


**Figure 2. Design Model Data Flow**

Thrust and specific fuel consumption are calculated in the *propulsion* discipline, which at this time is simply a look-up table for each of these values based on flight speed and altitude. In the future, this will be updated to consider different size engines during the design cycle such that engine weight and nacelle drag may also be treated as variables.

The heart of the design model is an open-source 6-DoF flight simulator called JSBSim,[16] modified to run in batch mode as an S-Function in Matlab's Simulink.® The development of JSBSim began over a decade ago with Berndt,[16] and over the years has grown into a major project involving dozens of engineers. It is quite powerful as a means of evaluating aircraft flight dynamics and includes the means for fully configuring the flight control system, propulsion, aerodynamics, and landing gear of any general aircraft. This is typically done through a front-end *.xml* input file, where the aircraft's characteristic parameters are read in once at the onset of the simulation and then control inputs are treated as dynamic properties updated several times per second during run-time. Mills[17] began work on the basic implementation of the S-Function over a year ago and the authors continued its further development for the work presented in this paper. This development included modifications to the flight simulation engine itself, changes to the code ($C^{++}$) enabling the effects of nearly all aircraft design variables to be treated as dynamic properties in the same way as control inputs, such that they can be varied as a functions of time during the execution of the flight model in Simulink. This makes possible the rapid evaluation of a very wide range of aircraft performance parameters for a nearly limitless number of aircraft configurations.

## B. Aircraft Model

To demonstrate the multi-state design problem, the analysis begins with the baseline configuration of a Beechcraft Super King Air Model 200, as shown in figure 3. This aircraft was chosen because its behavior is well understood and there is ample geometry data which is publicly available. Additionally, the primary author has spent time flight testing real-world versions of it, most notably the Air Force modified C-12C, to which this particular computational model was calibrated. The C-12C version is powered by two Pratt and Whitney PT6A-41 turboprop engines, each rated at 850 horsepower (sea level), and has a fully reversible flight control system. In addition, it is equipped with a rudder boosted yaw damper system.

Care was taken to ensure that results from the vortex lattice analysis and from flight simulation were representative of the real-world aircraft. Thus, comparisons were made to flight test validated data taken

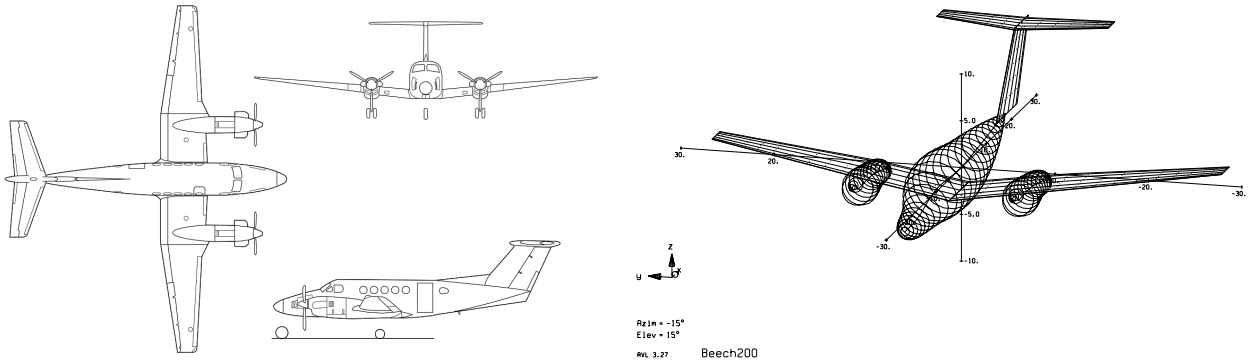


(a) 3-View (public domain)

(b) AVL Representation

**Figure 3. Beechcraft Super King Air Model 200**

from an in-flight performance evaluation of the Beech C-12C performed at Edwards AFB, CA, in 2001.[18] As an example of one such comparison, figure 4 shows that the computed and flight test validated drag polars match up closely. Since such comparison are not always possible for aircraft of new design, this is yet another advantage of starting the multi-state analysis from a known baseline vehicle. The authors contend that the bounds of the validated analysis should extend well beyond the ±10% perturbations described in the next section.

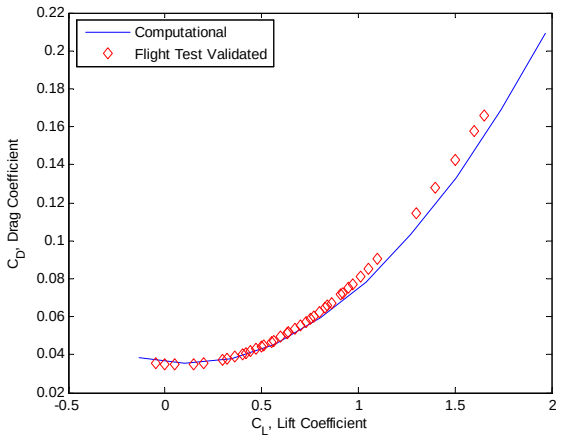


**Figure 4. Drag Polar Comparison**

## IV. Multi-State Test Case

As mentioned earlier, the purpose of this initial research stage was to examine the relationship between an aircraft's global design variables and its performance output for differing aircraft states. This may then be used to evaluate the expected performance and availability of the system across various time periods and subject to changes in component or element *mean-time between failures (MTBF)*. The following introduces a simple multi-state test case applied to the evaluation of an aircraft's climb and turn capability in the face of several selected failures.

### A. Markov Model

The number of failure cases and all of their permutations can be quite large in any particular multi-state analysis. Here, we chose to limit failures to those most directly affecting performance and dynamics, specifically failure of the rudder, ailerons, and/or a single engine. These correspond to the failure rates $\lambda_R$, $\lambda_A$, and $\lambda_E$, respectively. Failure rates were set at values of $2e^{-6}$ failures per hour for the rudder and ailerons and $8e^{-6}$ failures per hour for the engine, which was then doubled since only the possibility of losing one engine was considered. If sequence dependence is ignored, this leaves only seven failed plus one nominal system configurations to consider. This is depecited in the aggregated Markov model shown in figure 5. This model appears somewhat different than that shown in figure 1 because several of the downstream states can now be reached from multiple upstream states due to the aggregation. The solution of the model in order to determine each state probability $p_k$, however, is performed in the same manner.

The states in the aggregated Markov model are:

- *State N*: nominal configuration, no failures – turn controlled with ailerons
- *State 1*: left engine failed, rudder and ailerons functional – turn controlled with ailerons
- *State 2*: rudder failed, ailerons and engines functional – turn controlled with ailerons
- *State 3*: ailerons failed, engines and rudder functional – turn controlled with rudder
- *State 4*: left engine and ailerons failed, rudder functional – turn controlled with rudder
- *State 5*: left engine and rudder failed, ailerons functional – turn controlled with ailerons
- *State 6*: rudder and ailerons failed, engines functional – turn controlled with differential thrust
- *State 7*: left engine, rudder, and ailerons failed – no control

For the analysis of the Markov model and calculation of state probabilities $p_k$, two time periods were used. The first was a typical mission duration of 8 hours and the second was a 20,000-hour time period providing an indication of problem areas that might manifest themselves over the system lifetime. Results for both time periods are provided in Section V.

### B. Aircraft Performance Metrics

The function of interest is cast as *expected* specific excess power in a turning climb, which must be evaluated for the nominal condition *and* each of the failure states in order to compute equation 2. Realistically, the system availability given by equation 1 would also be important to designers in terms of a measure of performance, but this is not a continuously differentiable function as jumps occur whenever a state's performance $G_k$ crosses the threshold set by $W_M$. We assume for now that increasing expected performance $E_G$ should positively correlate with increasing system availability $E_A$, thus making it possible to better pinpoint changes in regions where that threshold is not crossed. This specific excess power, $P_s$ can be computed one of two ways; first, from the analytical equation $P_s = (T - D)V/W$ using the proper thrust ($T$) and drag ($D$) increments for the various failure modes, or from the flight simulation code mentioned above using the outputs $dh/dt$, $dV/dt$, and $V$ to compute specific excess power from $P_s = dh/dt + (V/g)(dV/dt)$. The latter method was used for this study to better capture the dynamic effects of the state changes. The expected performance equation resulting from this formulation is given in equation 3,

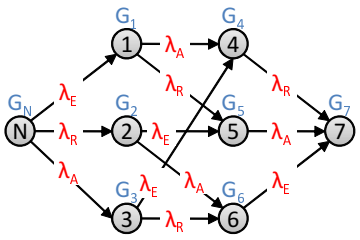


**Figure 5. Problem Specific Markov Chain**

$$E_G(\bar{\lambda}, \bar{x}) = \sum_{k=1}^{8} p_k(\bar{\lambda}) P_s(\bar{x})_k = \sum_{k=1}^{8} p_k(\bar{\lambda}) [\dot{h}(\bar{x}) + \frac{V(\bar{x})}{g} \dot{V}(\bar{x})]_{avg,k} \tag{3}$$

where $\bar{\lambda}$ and $\bar{x}$ are vectors of design variables, $g$ is the gravity constant, and the *avg* subscript indicates the values are averaged over the last ten seconds of the simulation, allowing the aircraft a chance to stabilize before the performance metric is computed.

Each simulation is run for a period of ninety seconds (accelerated in batch mode), beginning from a full-throttle, constant velocity climbing turn at 15° of positive bank (to the right). Initial conditions are set at an altitude of 5000 ft. and a velocity of 140 knots, which is close to the best speed for a cruise climb

in the Beech 200. Simple proportional-integral-derivative (PID) controllers are used to maintain airspeed (elevator channel), bank (channel dependent on failure state), and yaw (rudder or throttle channel according to state). Engine failure is modeled by cutting the throttle to zero after ten seconds and control failures disallow the use of the control surface throughout the simulation, assuming that it is stuck in the neutral position. In the case of the engine failure, the model accounts for the additional drag effects of the feathered prop and the nacelle.

### C. Aircraft Geometry

Rather than perform the full re-optimization of an existing aircraft, at this stage we are interested in identifying those elements that might drive system loss probability through sensitivity analysis. Therefore, a subset of aircraft geometry variables were selected and their values perturbed by ±10%. These variables and their values are given in table 1. Baseline values correspond to those of the aircraft in figure 3(a).

**Table 1. Aircraft Geometry Perturbations**

| Design Variable: | Low Value | Baseline | High Value |
|---|---|---|---|
| Wing Area | 272.7 $ft^2$ | 303 $ft^2$ | 333.3 $ft^2$ |
| Wing Span | 49.05 $ft$ | 54 $ft$ | 59.95 $ft$ |
| Horizontal Tail Area | 65.7 $ft^2$ | 73 $ft^2$ | 80.3 $ft^2$ |
| Horizontal Tail Span | 16.51 $ft$ | 18.3 $ft$ | 20.17 $ft$ |
| Vertical Tail Area | 105.12 $ft^2$ | 116.8 $ft^2$ | 128.48 $ft^2$ |
| Vertical Tail Height | 7.5 $ft$ | 8.33 $ft$ | 9.16 $ft$ |
| Spanwise Engine Location | 7.72 $ft$ | 8.58 $ft$ | 9.44 $ft$ |
| Aileron Chord* | 15.3% | 23% | 30.7% |
| Elevator Chord* | 35.1% | 41% | 46.9% |
| Rudder Chord* | 38.4% | 44% | 49.6% |
| Wing Sweep | 0 deg | 4 deg | 15 deg |

* Given in percent of wing, horizontal tail, or vertical tail chord.

## V. Results

Each geometry perturbation in table 1 was run for each Markov state, this included one baseline geometry plus eleven low values and eleven high values for a total of 23 geometric cases. This resulted in 184 simulation runs when applied to the eight Markov states. Total computational time was approximately 11.5 minutes when split across two processors on a laptop with an Intel Core 2 Duo 2.5GHz CPU and 3.0GB of RAM (each simulation run takes approx. 7 seconds). For future execution in an optimization process it is expected that certain design-of-experiment techniques and approximation models might be used to reduced the amount of function calls to the simulation engine. In addition, classic Multidisciplinary Design Optimization (MDO) techniques such as System Sensitivity Analysis could be used to reduce the total number of function calls.

### A. Multi-State Aircraft Performance

To best show the effects of each geometry case on the performance metric, the scatterplots in figure 6 were constructed, plotting the average values of bank angle vs. specific excess power for each state. Each plot contains 23 geometric cases, with the baseline geometry case marked by dashed lines. Note that several cases may overlap, thus not all 23 instances are discernible on each plot. The output of cases which resulted in loss of aircraft was observed to correspond, without exception, to values of $P_s$ less than -1000 ft/min, often much less. Thus, these cases were filtered and their values set to a bank angle of zero and a $P_s$ of -1000 ft/min in order to show them uniformly on the scatterplots.

Of the 184 cases, 27 resulted in loss of the aircraft. Twenty-three of these came from state 7, which was to be expected since there was no way to control the aircraft without use of rudder, aileron, or differential thrust. Two cases came from the analysis of state 4, where the left engine and ailerons were failed, requiring

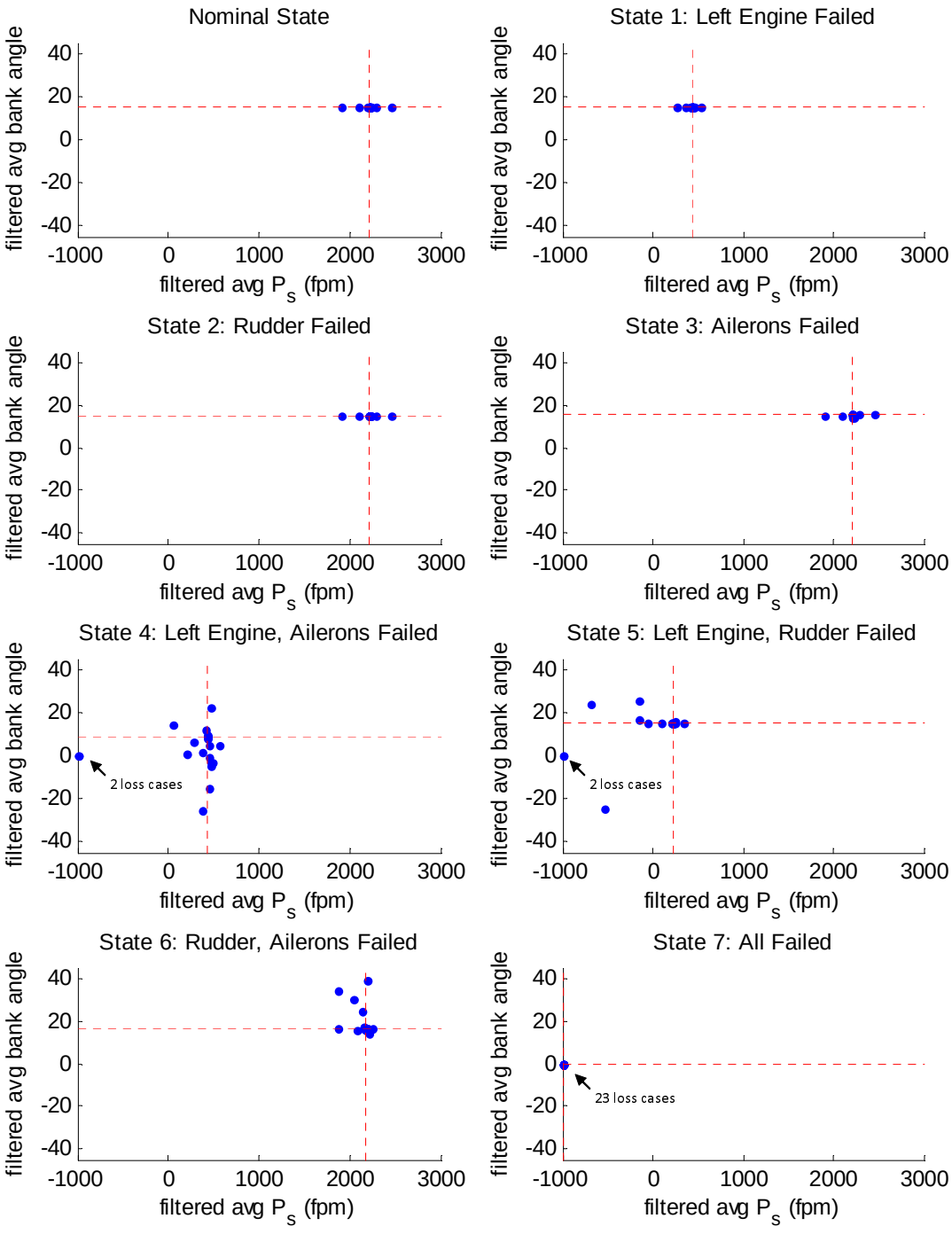


**Figure 6. Effect of Geometry Perturbation on $P_s$ vs. Bank Angle for Each Markov State**

bank angle and turn to be controlled with only the rudder in the face of asymmetric thrust. The remaining two cases came from state 5, with the left engine and rudder failed and bank angle controlled with ailerons.

The failing geometries of state 4 were those with the vertical tail height decreased by 10% and the spanwise engine location at the greatest distance from the fuselage. Experimentation with the control scenarios for this state as well as several weeks of flight testing an actual Beech 200 aircraft (many years prior to this) led the authors to suspect that an unsatisfactory Dutch roll mode might be to blame. Indeed, inspection of the control derivatives showed that these two geometries had the lowest values for $|C_{n\beta}/C_{l\beta}|$ of all 23 cases. A general rule in aircraft design is that $|C_{n\beta}/C_{l\beta}|$, which is a measure of the aircraft's lateral stability in relation to its directional stability, should be greater than 0.33. For the case with the reduced tail height, this value was 0.08 and for the outboard engine placement it was 0.12.

There are a couple items to note concerning this finding. First, the baseline aircraft has $|C_{n\beta}/C_{l\beta}| = 0.22$, which is less than the threshold given above. This is a known characteristic of the the Super King Air Model 200 and one of the reasons why the aircraft is equipped with a rudder boosted yaw damper. Second, in five of the eight states, these poor Dutch roll characteristics did not result in a loss of the aircraft (one of the failed cases in state 5 was also the shortened tail geometry). However, in the adverse circumstances presented by state 4, the rudder was unable to dampen the Dutch roll mode while also being required to control bank angle in a turning climb. While it may be argued that this particular outcome is specific to the scenario and control laws presented here, it does demonstrate the emergence of critically negative behavior in off-nominal conditions that can be affected by small changes in geometric design variables.

The tendency for larger amplitude Dutch roll is also seen in the case with higher wing sweep (which typically results in lower $|C_{n\beta}/C_{l\beta}|$), as seen in figure 7 for state 6. Here the mode is largely undamped as differential thrust is used to maintain the 15° bank angle.

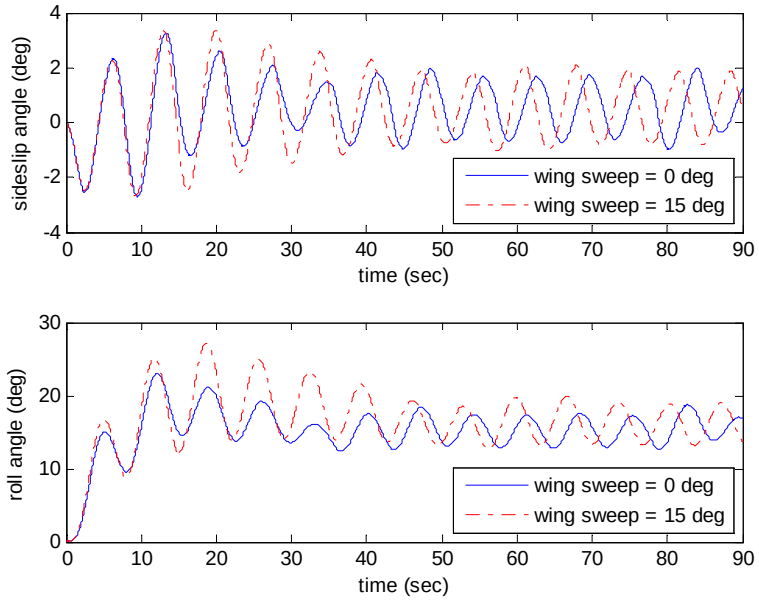


**Figure 7. Sideslip and Roll Angle Oscillations in State 6**

## B. Expected Performance Sensitivity Analysis

It is important to determine which parameters have the greatest effect on the overall system performance. As mentioned earlier, the expected performance in equation 2 tends to treat the Markov state probabilities as "weights." Thus, given sufficiently low failure rates, a short Markov time period will tend to have expected performance values nearly identical to the nominal state. As the overall system lifetime increases, the expected system performance will change as probability increases. To illustrate this, consider an 8-hour mission and a 20,000-hour system lifetime, both typical for this type of aircraft. If no repairs are made to

the system, the Markov state probabilities will be as in the first two columns of table 2, given the failure rates mentioned earlier. Even if repairs are considered, these values provide some indication of the amount of resources that must be allocated towards maintenance. While the third column in table 2 is not necessary applicable to this aircraft, it is included to emphasize the impact of this type of analysis on a system expected to operate for long periods of time in a austere environment, for instance an ultra long endurance UAS with a continuous mission duration of 5 years.[19]

**Table 2. Markov State Probabilities**

| Markov State | 8-Hour Sortie | 20,000-Hour System Lifetime | 5-Year Sortie |
|---|---|---|---|
| Nominal | 99.9% | 67.0% | 41.6% |
| State 1 | 0.01% | 25.3% | 42.3% |
| State 2 | $< 0.001\%$ | 2.7% | 3.8% |
| State 3 | $< 0.001\%$ | 2.7% | 3.8% |
| State 4 | $< 0.001\%$ | 1.0% | 3.9% |
| State 5 | $< 0.001\%$ | 1.0% | 3.9% |
| State 6 | $< 0.001\%$ | 0.1% | 0.35% |
| State 7 | $< 0.001\%$ | 0.04% | 0.35% |

Given these probabilities, it is possible to determine the expected system performance. More importantly, one may solve the expected performance sensitivity for the 8-hour sortie and 20,000-hour system lifetime. In this case, the sensitivities are simple perturbations from the baseline value - the expected performance sensitivity for the geometric values are figured from a central difference given the high and low variations from table 1. In addition, forward differences are made for perturbations to the individual component failure rates (aileron, rudder, and engine), also varied by 10%. The sensitivities for the 8- and 20,000-hour expected specific excess power are shown in figure 8.

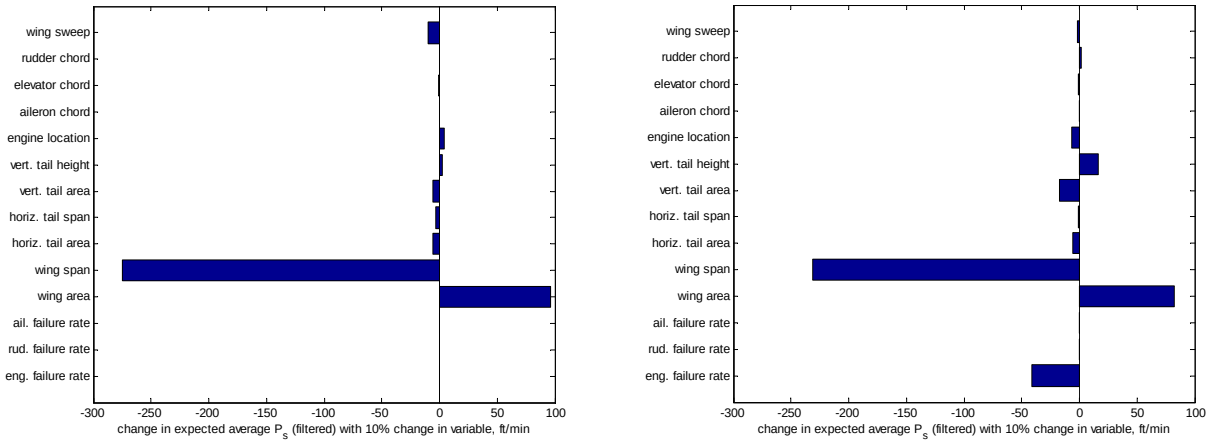


(a) 8-hour

(b) 20,000 hour

**Figure 8. Comparison of Sensitivities**

As expected, the 8-hour sortie looks much like a traditional, nominal aircraft sensitivity analysis for specific excess power should. Here, wing span is the most sensitive component; this is due to the large change in wing weight due to variations in aspect ratio. Wing area is the next highest contributor, this time because of the effect of increased wing loading (smaller wing) on reduction in wing weight.

Results change marginally for the 20,000-hour system lifetime sensitivity. Wing span and area remain the most influential variables; this is to be expected given that the nominal state still has a 67% probability and thus retains a significant influence. However, previously insensitive variables are now more prominent.

These are, in order, engine failure rate, vertical tail area, vertical tail height, spanwise engine location, and horizontal tail area. The first, engine failure rate, comes as little surprise given the relatively high probability of an engine failure (Markov states 1, 4, 5, and 7), which adds up to 27.3% per table 2. Hence, reducing engine failure rate would, naturally, have a beneficial effect on the expected specific excess power.

Others may seem less obvious. The spanwise engine location has an influence on expected specific excess power because the larger moment available to engines placed further apart means that less differential thrust is needed to help with turning in the event of an aileron failure. Conversely, engines placed closer suffer a reduced trim drag penalty during engine failure cases. The higher probability of engine failure leads to the overall negative impact of moving the engines further outward. The vertical tail height is an interesting case - in particular, it has been noted that the aircraft's yaw stability requires a yaw damper in the nominal case. Increasing the vertical tail span helps to increase directional stability, especially in cases where there is rudder or engine failure. As mentioned earlier, smaller wing sweep decreases lateral stability (the denominator of $|C_{n\beta}/C_{l\beta}|$) during both nominal and off-nominal conditions, which can improve Dutch roll characteristics as well.

Hence, it seems that it may be possible to use expected performance sensitivity analysis in conjunction with standard, nominal-case sensitivity analysis to both improve a system design and increase its robustness. In particular, expected performance sensitivity could be used to find those variables that are insensitive in the nominal case but highly sensitive in the expected case. These would be prime candidates for exploitation to ensure that off-nominal system performance is improved at little to no expense to nominal performance.

## VI. Conclusion

The results of this study provide promising evidence as to the utility of expected performance analysis and its ability to provide design engineers with data to generate more robust solutions early in the design process. Future work will expand the expected performance sensitivity analysis experiments. The design structure matrix (DSM) format of the system model lends itself to MDO-type sensitivity decomposition, which could greatly reduce the computational effort to generate these global sensitivity values. Once these methods have been validated for this relatively straightforward aircraft design problem, it will be necessary to apply it to a larger, less understood model.

In summary, a multi-state design model approach was introduced that enables the rapid and flexible analysis of multi-state aircraft performance. Some key enablers of this approach are a medium-fidelity flight simulation engine integrated directly into the design process loop and the streamlined computation of aircraft weights, inertias, aerodynamics, and stability & control parameters from a comprehensive set of traditional design variables. This provides the ability to evaluate the full spectrum of performance parameters for each design across a range of aircraft (failure) states. Coupled with a Markov analysis to solve for state probabilities, this is a very powerful approach to early-stage development of complex and long-lifetime systems such as aircraft.

## References


[1]Cessna, "News Releases: Cessna Skycatcher to Re-Enter Development Program," http://www.cessna.com/NewReleases/New/NewReleaseNum-1192268569074.html, Accessed March 2010.

[2]Steinberg, M., "Historical Overview of Research in Reconfigurable Flight Control," *Journal of Aerospace Engineering*, Vol. 219, No. 4, 2005, pp. 263–275.

[3]Burcham, F. W., Maine, T. A., Fullerton, C. G., and Webb, L. D., "Development and Flight Evaluation of an Emergency Digital Flight Control System Using Only Engine Thrust on an F-15 Airplane," Tech. rep., NASA, Edwards, CA, Sept. 1996.

[4]Monaco, J. F., Ward, D. G., and Bateman, A. J., "A Retrofit Architecture for Model-based Adaptive Flight Control," AIAA 2004-6281, 1st AIAA Intelligent Systems Technical Conference, Chicago, IL, Sept. 2004.

[5]Babcock IV, P. S. and Zinchuk, J. J., "Fault-Tolerant Design Optimization: Application to an Underwater Vehicle Navigation System," Tech. rep., IEEE/OES Symposium on Autonomous Underwater Vehicles, Washington, D.C., June 1990.

[6]Babcock IV, P. S., "Developing the Two-Fault Tolerant Attitude Control Function for the Space Station Freedom," Tech. rep., 20th International Symposium on Space Technology and Science, Gifu, Japan, May 1996.

[7]Babcock IV, P. S., "An Introduction to Reliability Modeling of Fault-Tolerant Systems," CSDL-R-1899, The Charles Stark Draper Laboratory, Inc., Cambridge, Massachusetts, Sept. 1986.

[8]Dominguez-Garcia, A. D., Kassakian, J. G., Schindall, J. E., and Zinchuk, J. J., "On the Use of Behavioral Models for the Integrated Performance and Reliability Evaluation of Fault-Tolerant Avionics Systems," Tech. rep., IEEE/AIAA Digital Avionics Systems Conference, Portland, Oregon, Oct. 2006.

[9]Dominguez-Garcia, A. D., *An Integrated Methodology for the Performance and Reliability Evaluation of Fault-Tolerant Systems*, Ph.D. thesis, Massachusetts Institute of Technology, Cambridge, Massachusetts, June 2007.

[10]Dominguez-Garcia, A. D., Kassakian, J. G., Schindall, J. E., and Zinchuk, J. J., "An Integrated Methodology for the Dynamic Performance and Reliability Evaluation of Fault-Tolerant Systems," *Journal of Reliability Engineering and System Safety*, Vol. 93, No. 11, 2008, pp. 1628–1649.

[11]Borer, N. K., Claypool, I. R., Clark, W. D., West, J. J., Odegard, R. G., Somervill, K. M., and Suzuki, N. H., "Model-Driven Development of Reliable Avionics Architectures for Lunar Surface Systems," Tech. rep., IEEE Aerospace Conference, Big Sky, Montana, March 2010.

[12]Levitin, G. and Lisnianski, A., "A New Approach to Solving Problems of Multi-State System Reliability Optimization," *Quality and Reliability Engineering International*, Vol. 17, No. 2, 2001, pp. 93–104.

[13]Brandt, S. A., Stiles, R. J., Bertin, J. J., and Whitford, R., *Introduction to Aeronautics: A Design Perspective, second edition*, American Institute of Aeronautics and Astronautics, Reston, VA, 2004.

[14]Raymer, D. P., *Aircraft Design: A Conceptual Approach, third edition*, American Institute of Aeronautics and Astronautics, Reston, VA, 1999.

[15]AVL, "Athena Vortex Lattice Solver," http://web.mit.edu/drela/Public/web/avl/, Accessed March 2010.

[16]Berndt, J. S., "JSBSim: Open Source Flight Dynamics Model in C++," http://jsbsim.sourceforge.net/JSBSimFlyer.pdf, Accessed March 2010.

[17]Mills, B., "DIY Drones: Profile of Brian Mills," http://diydrones.ning.com/profile/BrianMills, Accessed March 2010.

[18]Thompson, S. and Agte, J., "C-12C Aerodynamic Model Evaluation, USAF TPS Memorandum," Tech. rep., U.S. Air Force Test Pilot School, Edwards AFB, CA, April 2001.

[19]DARPA, "Vulture Program: Broad Agency Announcement (BAA) Solicitation 07-51," Defense Advanced Research Projects Agency TTO, July 2007.